Automated Three-Stage Nucleus and Cytoplasm Segmentation of Overlapping Cells

Afaf Tareef[1], *Student Member, IEEE*, Yang Song[1], *Member, IEEE*, Weidong Cai[1], *Member, IEEE*, David Dagan Feng[1], *Fellow, IEEE*, and Mei Chen[2], *Member, IEEE*

[1]Biomedical and Multimedia Information Technology (BMIT) Research Group, School of Information Technologies
University of Sydney
NSW 2006, Australia

[2]Intel Science and Technology Center on Embedded Computing
Carnegie Mellon University
Pittsburgh, PA 15213, USA

***Abstract*— Developing segmentation techniques for overlapping cells has become a major hurdle for automated analysis of cervical cells. In this paper, an automated three-stage segmentation approach to segment the nucleus and cytoplasm of each overlapping cell is described. First, superpixel clustering is conducted to segment the image into small coherent clusters that are used to generate a refined superpixel map. The refined superpixel map is passed to an adaptive thresholding step to initially segment the image into cellular clumps and background. Second, a linear classifier with superpixel-based features is designed to finalize the separation between nuclei and cytoplasm. Finally, edge and region based cell segmentation are performed based on edge enhancement process, gradient thresholding, morphological operations, and region properties evaluation on all detected nuclei and cytoplasm pairs. The proposed framework has been evaluated using the ISBI 2014 challenge dataset. The dataset consists of 45 synthetic cell images, yielding 270 cells in total. Compared with the state-of-the-art approaches, our approach provides more accurate nuclei boundaries, as well as successfully segments most of overlapping cells.**

Keywords— Cervical overlapping cells, Pap smear images, Support vector machine, Edge and region integration, Morphological reconstruction, Cell segmentation.

I. INTRODUCTION

Cervical cancer is one of the major causes of cancer death in females worldwide. The Papanicolaou test (abbreviated as Pap smear or Pap test) is the most effective screening test used to detect the cervical pre-cancerous and cancerous changes in a sample of cervical cells based on the shape variations of the nuclei and cytoplasm. Pap test has drastically changed the prognosis of women with cervical cancer as it has proved its ability to detect 95% of the cancers of the vaginal neck [1]. In the test, a sample of cells from the uterine cervix smeared onto a microscope slide needs to be analyzed for examination. Due to the complex background, the complexities of cell structures, and existence of overlapping cells, automated analysis is still an open problem. One of the most critical challenges in this procedure is the delineation of the overlapped cells.

Although there are many segmentation techniques proposed for cervical cell segmentation, the majority of them cannot undertake a complete nucleus and cytoplasm segmentation. The current cervical cell segmentation literature can be classified into four main categories: techniques to segment the nuclei and cytoplasm of single cervical cells (i.e., isolated or free-lying cells without any overlapping with the other cells) [1, 2], techniques to segment overlapping nuclei [3-7], techniques to segment overlapping nuclei plus the whole cellular regions of overlapping cytoplasm [8, 9], and only recently some techniques to completely segment the overlapping nuclei and cytoplasm [1, 10].

The initial researches in segmentation of cervical microscopic images were mainly based on thresholding techniques [11]. Then, many techniques were proposed based on active contour or snakes [2, 3], edge detectors [12, 13], watershed [8, 9], and region growing techniques [14] to optimize the segmentation results. In [2], a free-lying cells segmentation technique is introduced by Li et al. The segmentation process involves k-mean clustering to initially cluster the cell into nucleus, cytoplasm, and background, and then Radiating Gradient Vector Flow (RGVF) Snake is performed to finalize the segmentation.

Some of the techniques proposed to segment the overlapping nuclei can be found in [3-7]. In [3], a segmentation technique based on an improved active contour model that is separately built for each nucleus is introduced. Another overlapping nuclei segmentation technique is introduced in [7] based on morphological reconstruction. Regarding the third type of segmentation techniques, an unsupervised approach for the segmentation of overlapping nuclei and cellular clumps of cervical cells is proposed in [8]. Automatic thresholding, morphological operations, multi-scale hierarchical watershed segmentation algorithm, and binary classification are applied to separate the nuclei and cellular clumps from the background. Another nuclei and whole cytoplasm segmentation technique is presented in [9]. In this technique, multi-scale watershed segmentation technique is used to initially segment the image, and then, support vector machine is utilized on some previously selected regions based on the homogeneity and circularity properties.

Recently, Béliz-Osorio et al [1] have proposed a new technique for the segmentation of overlapping cervical cells

based on locally constrained watershed transform. Their results proved that this type of watershed can be used to segment nuclei and cytoplasm in overlapped cells. However, it is often inaccurate in case of large overlapping area. In [10], a novel nucleus and cytoplasm segmentation technique based on joint level set optimization is introduced. In this technique, each nucleus, detected by Maximally Stable External Regions (MSER) algorithm, forms a separate level set function. This technique provides reasonably accurate segmentation, and successfully segments most of the overlapping cells. Hence, this approach will be used as a benchmark to evaluate the performance of our proposed one.

In this paper, an automated three-stage cervical cell segmentation technique based on edge and region integration is proposed to accurately segment both the nuclei and cytoplasm of overlapping cells. The rest of this paper is organized as follows: Section II describes the details of the proposed segmentation approach. In Section III, the material and evaluation methods are introduced. Simulations and analysis of the performance of the approach are presented in Section IV. The conclusion is drawn in Section V.

II. Overlapping Nucleus and Cytoplasm Segmentation Approach

The aim of cervical cell segmentation is to categorize the overlapping cells into background, nucleus and cytoplasm of individual cells. Our proposed segmentation approach achieves this goal by three main stages: (1) cellular clump detection stage including superpixel clustering and thresholding steps; (2) nuclei detection and segmentation stage based on support vector machine; and (3) overlapping cell segmentation stage based on edge enhancement procedure, gradient thresholding, morphological operations and region properties evaluation. The various stages of our proposed technique are illustrated in Fig.1.

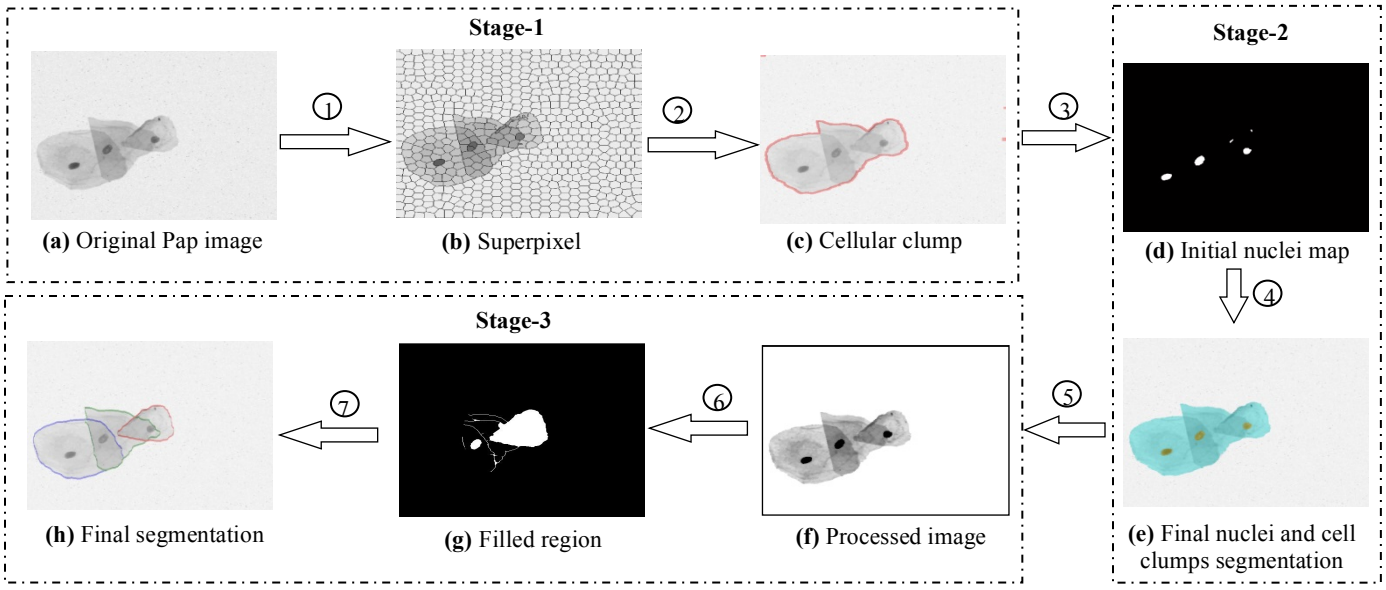

Figure 1. Procedure for the proposed three-stage approach. Stage-1: (1) SLIC oversegmentation and generation of a refined superpixel map, (2) adaptive thresholding to separate the cellular clump from the background, (3) initial detection of the nuclei using thresholding with threshold=0.5; Stage-2: (4) finalizing the segmentation of nuclei and cytoplasm regions with SVM, (5) preprocessing for the last stage: removing the background and equalized the cellular clumps based on the SVM results; Stage-3: (6) performing morphological operations on the edges maps extracted by Otsu's thresholding on the Sobel gradient of the processed image, (7) region evaluation for finding the optimal cytoplasm map.

A. *Cellular clumps segmentation based on simple linear iterative clustering and adaptive thresholding*

In order to highlight the cellular clumps and reduce the searching area in the image, Simple Linear Iterative Clustering (SLIC) algorithm [15] is performed to generate an over-segmented superpixel map. With superpixels, the image is segmented into local and coherent clusters containing statistically homogenous regions. The median value for each superpixel provides a good description for the content of the superpixel. The median values are thus calculated to generate a refined superpixel map where the background and cellular clumps are quite different. Due to the continuous intensity variation from one image to other, a threshold adaptive to the local intensity variations and region evaluation on the obtained superpixel map is used to separate the free-lying cells, cellular clumps, and background. Fig. 1 (b) shows the results of over-segmentation of the original example image (shown in Fig. 1 (a)) using SLIC, with 0.01 regularization factor and 20-pixels superpixel size, after replacing the superpixels intensity values by the median values. Fig.1 (c) shows the cell clump boundaries using thresholding technique. As noticed, there is a minor false positive detection on the image boundary.

B. *Nuclei detection and segmentation based on linear support vector machine*

In this stage, Support Vector Machine (SVM) with linear kernel is used to finalize segmentation of image components.

SVM has been widely used in cell image analysis to solve the complex segmentation problems [16, 17, 18, 19].

To facilitate the nuclei detection and segmentation, this stage focuses on the foreground segmented in the previous stage. The histogram of the region of interest (i.e., foreground) is equalized to emphasize and highlight the details. In general, the histogram equalization increases the global contrast of whole image, and since the contrast of background in Pap smear images seems quite close to some part of the cytoplasm, applying histogram equalization in earlier stage would increase the false positive detection rate.

After obtaining a clear cytoplasm clump from the previous step, the nuclei detection and segmentation are performed. We perform the detection and segmentation by first highlighting the dark regions, which most likely are nuclei, of the processed image, and then running SVM classifier based on eight superpixel-based features to obtain refined results.

A thresholding technique with threshold=0.5 is chosen to be our initial highlighting method, and then the dark regions with elongated shape are ignored. The sample results are shown in Fig. 1(d). In practice, even after ignoring the elongated regions, this step cannot always succeed in detecting the accurate nuclei boundary. In other words, there are pixel-based false negative and object-based false positive detections in the obtained results (e.g., dark details in cytoplasm appear as a nucleus, and some or all nucleus pixels are labeled as a cytoplasm). However, the obtained map, which is used as a feature in the next step, is still useful to get more accurate results than directly utilizing SVM. A supervised SVM classifier with three classes (i.e., background, cytoplasm, and nuclei) is then applied to finalize the separation of nuclei from cytoplasm within the cell regions, to correct the false positive detections in the background segmented in the previous stage, and to optimize the pixel-based and object-based nuclei segmentation accuracy.

In general, nuclei are distinguished by low intensity value comparing with its neighbor, homogenous texture, and circular shape. Therefore, a set of texture and contour features as well as comparative features are extracted from each superpixel. There are eight superpixel-based features extracted from each superpixel. One of the features that significantly improves the performance of segmentation is the intensity value of each superpixel in the intensity scaled image. In order to increase the intensity difference between the superpixels, the intensity values are rescaled to a new range which is equal to the number of superpixels. The median value for each superpixel is used to describe the new intensity values.

Another feature that can effectively discriminate nuclei from the cytoplasm is the object shape information represented by the local edge orientation histogram (EOH) [20, 21]. The histogram of edges in each direction (horizontal, vertical directions, and the diagonals) is locally calculated for each superpixel, as well as the number of whole edges using Sobel edge detection operator to give a good description of the shape. In addition, gray level co-occurrence matrix (GLCM) homogeneity and contrast features, the difference between each superpixel and its neighbors, the standard deviation and the most frequent intensity value in each superpixel, and finally a label indicating the initial segmentation for each superpixel, are extracted. After composing the features vectors for all superpixels, the linear SVM is used to get the final segmentation. At the end of this stage, based on the results of SVM as shown in Fig. 1(e), a new version of the image is generated by ignoring the detected background. The processed image is saved to be the input of the final stage.

C. Overlapping cervical cell segmentation based on gradient thresholding, edge and region integration

The goal of this stage is to delineate the boundary of both free-lying and overlapping cells on all detected nuclei and cytoplasm pairs. This process is started by equalization and denoising processes. Gradient thresholding is used to extract two groups of edge map: simple edge map and detailed edge map. Then, the overlapping cells are segmented based on the edge maps, morphological operations, and region properties.

First, a preprocessing procedure is applied to enhance the images. In order to highlight the contour details, histogram equalization is applied on the input image. Then, the gradients of the processed image are computed and passed to automatic Otsu's thresholding method to get a simple edge map. Fig. 2 (a) and (b) show the enhanced image and the corresponding gradients.

To obtain the detailed edge map, more processes are taken before thresholding. First, the Antistrophic Diffusion Filter (ADF) (with k=0.08 and three iterations) is applied to remove noises and unnecessary details while preserving the important information in the image (e.g., edges). The obtained denoised image is equalized to sharpen the edges, and then Otsu's thresholding is applied on the gradient of the denoised and equalized image.

In order to get connected and linked edges, closing morphological process (using a disk with radius equals 2) is performed with isolated pixels removed on both edges maps. The outputs of this step are clear and semi-connected edges maps as shown in Fig. 2 (c) and 2 (d).

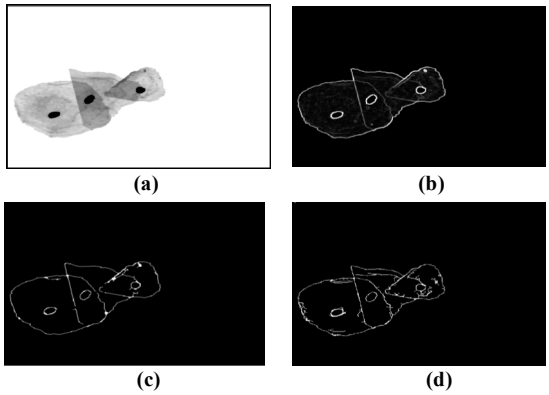

Figure 2. (a) The enhanced image, (b) the corresponding gradient, (c) the edges map, and (d) simple the detailed edges map.

The reason behind generating two maps of edges is to obtain good segmentation for different types of cells. In case of single and semi-single cells, the simple edge group gives more accurate segmentation where the boundary of each cell is clear, whereas using detailed edges in this case may divide the cell into small parts or accepting part of the attached cell as a part of the cell in focus. On the other hand, the simple edge group is unable to segment the cells with a high overlapping rate as the inner edges of the overlapping cytoplasm are unclear or unconnected in the first group of edges.

After generating the edge maps, the region of interest for each nucleus is found with a fixed reasonable Euclidean distance from each nucleus where the nucleus is the center of the region of interest. A set of morphological operations is performed on both edges maps to obtain two solid and smooth cytoplasm maps. Specifically, morphological closing, thinning, filling, smoothing, and dilation are applied to clean up the segmented images. Closing operation is used to link the edges in the region of interest, thinning is applied to remove excess edges after connecting, and filling is performed to find the closed region of the connected pixels which represents the cytoplasm. Then, the filled region is smoothened by eroding the region twice with a flat and disk-shaped structuring element in order to remove any excess pixels connected to the cell boundary (i.e., a part of attached cell), and then, the remaining small and irregularly-shaped closed regions are filtered out. Finally, as smoothing operation inherently shrinks the filled region, dilation operation is performed to dilate the smooth region to finally get a more accurate cytoplasm map. The outputs from morphological operation are shown in Fig.3.

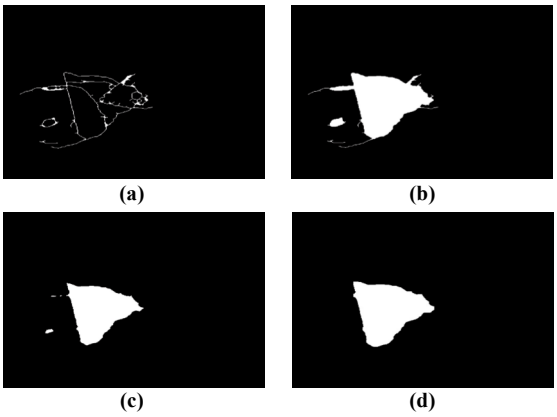

Figure 3. The output images of morphological operations. (a) the binary image after determining the region of interest with closing and thinning operations, (b) the output binary image after filling, (c) the smoothed image, (d) the final output after filtering and dilation.

In order to obtain the best segmentation result, the region properties of both cytoplasm maps are evaluated based on the circularity, area, eccentricity, and solidity properties; one of the obtained cytoplasm maps will be accepted (i.e., the one with the highest circularity value and acceptable area, eccentricity, and solidity value). The circularity shape property is calculated as:

$$Circ = \frac{4\,\pi\,\mathrm{A}}{P^2} \quad (1)$$

where A is the area of the region of interest and P is the perimeter.

In cases where both cytoplasm maps obtained in the previous steps were rejected, or the edges in the region of interest cannot be connected due to missing a large number of edge pixels, the proposed technique deals with these issues by carefully estimating the missing edges based on the existing clear and connected edges. Specifically, the region surrounding the nucleus that contains the largest number of edges is chosen to be our new region of interest, and by applying more detailed edge detection operator (i.e., Canny), the edges located in that region that are connected with the existing edges are used to get a closed region. Then, the same set of morphological operations applied in the previous step is applied on the obtained connected edges to get the cytoplasm map. This procedure can be iterated with different regions of interest until finding an acceptable cytoplasm map based on circularity, area, eccentricity, and solidity measures.

III. Material and Evaluation Methods

In this study, we used the ISBI 2014 'overlapping cervical cytology image segmentation challenge' dataset [22] for experiments. The dataset consists of 45 synthetic cell images, yielding 270 single and overlapping Pap cells in total. All images are gray-scale images with size of 512 × 512. The proposed approach underwent 2-fold cross evaluation.

To evaluate our approach, two sets of evaluation measures are used: object-based and pixel-based measures. The segmented region and the corresponding ground truth mask are used to classify the detected nuclei and cytoplasm as object-based true positive, false negative or false positive with respect to 0.7-threshold on the Zijdenbos similarity index (ZSI). ZSI is defined as the ratio of twice the overlapping area between the segmented region and the ground truth to the sum of both. It can be calculated as:

$$ZSI = \frac{2 \times |O_d \cap O_{gt}|}{|O_d| + |O_{gt}|} \quad (2)$$

where O_d represents the detected region, and O_{gt} represents the corresponding ground truth. The ZSI value that is greater than 0.7 indicates a good match between the two regions. Using the obtained object-based true positive (TP_O), false negative (FN_O), and false positive (FP_O) detection, precision (P) and recall (R) are computed as:

$$P = TP_O/(TP_O + FP_O) \quad (3)$$
$$R = TP_O/(TP_O + FN_O) \quad (4)$$

For pixel-based evaluation, the evaluation code provided by ISBI 2014 challenge [22] is used to compute the ZSI, pixel-based true positive (TP_P), pixel-based false negative (FN_P), and pixel-based false positive (FP_P).

IV. Experimental results and discussion

The experimental results of our approach are divided into two sections: nuclei segmentation results, and cytoplasm segmentation results. To evaluate the segmentation results of our approach, we used the results reported in ISBI 2014 challenge [22]. Note that the results in [22] were obtained using a larger dataset whose segmentation ground truths were only available to the challenge attendees while our results were based on the publicly available training set. Nevertheless, we believe the performance levels could be similar in both sets of images and we show the competitive performance of our method with these comparisons.

A. Nuclei segmentation results

Table I summarizes a comparison between our approach and three methods applied in [22]: Ushizima's segmentation approaches based on nuclear narrow-band seeding, graph-based region growing and Voronoi diagrams; Nostrati's approaches based on maximally stable extremal region detector (MSER), random decision forest classifier (RF), and signed distance map (SDM) function; and the segmentation technique proposed by Lu et al [10] based on a joint level set optimization using the results reported in the ISBI challenge. It is clear from the results that our approach outperforms the other up-to-date methods in terms of object-based detection. The proposed approach has achieved the highest object-based precision (0.989) and recall (0.959). In terms of pixel-based detection, the proposed approach achieved the highest recall (0.92) and ZSI value (0.926), whereas Ushizima's approach got the highest pixel-based precision value (0.96).

TABLE I. Nuclei segmentation results

	Precision (Object)	**Recall (Object)**	**Precision (Pixel)**	**Recall (Pixel)**	**ZSI (Pixel)**
Ushizima [22]	0.959	0.895	**0.968 ± 0.055**	0.871 ± 0.069	0.914 ± 0.039
Nostrati [22]	0.903	0.893	0.901 ± 0.097	0.916 ± 0.093	0.900 ± 0.053
Lu [22]	0.977	0.883	0.942 ± 0.078	0.912 ± 0.081	0.921 ± 0.049
Our proposed approach	**0.989**	**0.959**	0.943 ± 0.034	**0.920 ± 0.082**	**0.926 ± 0.047**

B. Cytoplasm segmentation results

Table II lists the cytoplasm detection and segmentation results using four measures; ZSI, object-level false negative cytoplasm detection (FNo), pixel-level true positive and pixel-based false positive detection. As shown in the table, our proposed approach has the highest pixel-based true positive detection (0.948) and ZSI coefficient (0.914), and the object-based false negative detection (0.296) is less than that obtained by Lu's technique (0.315). The false positive rate in our approach (0.005) is a little bit higher than other approaches, but it is reasonable due to the high object-based true positive detection of substantially overlapping cells using our approach. Based on the obtained results, the proposed approach has successfully separated most of the cells from the overlapping pairs.

TABLE II. Cytoplasm segmentation results

	FN (Object)	**TP (Pixel)**	**FP (Pixel)**	**ZSI (Pixel)**
Ushizima [22]	0.267± 0.278	0.841 ± 0.130	**0.002 ± 0.002**	0.872 ± 0.082
Nostrati [22]	**0.110 ± 0.166**	0.875 ± 0.086	0.004 ± 0.004	0.871 ± 0.075
Lu [22]	0.315 ± 0.294	0.905 ± 0.097	0.003 ± 0.005	0.893 ± 0.082
Our proposed approach	0.296 ± 0.277	**0.948± 0.059**	0.005 ± 0.007	**0.914± 0.075**

Figure 4 displays examples of the segmentation results with images of different overlapping rates. We divided the dataset into three sets: free-lying cells, double overlapping cells, and multiple overlapping cells. The segmentation results in case of free-lying and double overlapping cells are almost perfect segmentation. In the third set, despite of the blurring of the overlapped cytoplasm contours, the proposed approach can still effectively segment most of the cells. The best obtained pixel-based true positive detection rate was 0.98. Based on the results, the proposed technique has demonstrated a high ability to detect and extract both nuclei and cytoplasm of overlapping cells.

Finally, the average running time of our approach to segment each cell is 10 seconds using non-optimized MATLAB code on a PC Pentium i5 3.2 GHz and with 8 GB RAM. It is around 7 times faster than [10] where the average running time was 56 seconds per cell.

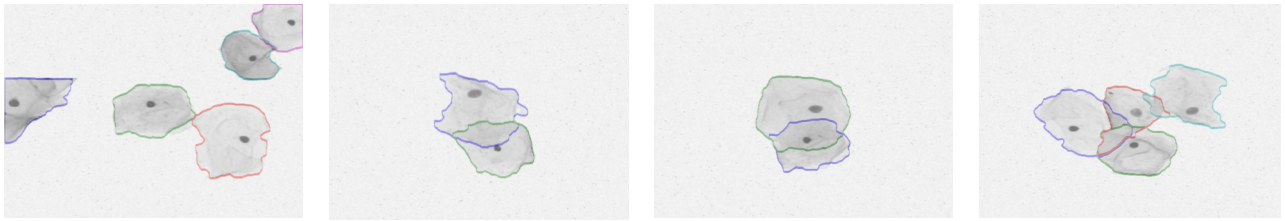

(a) (b) (c) (d)

Figure 4. Examples of the cytoplasm segmentation results (the contours are outlined by red, green, blue, cyan, yellow, gray, and purple color): (a) free-lying cells; (b, c) Double overlapping cells; and (d) multiple overlapping cells.

V. Conclusion

Automated segmentation of overlapping cervical cells poses a great challenge in the area of automated medical image analysis due to the noisy and complex background, non-homogeneous gradient, and the poor contrast of the cytoplasm. In this paper, a new approach for automated segmentation of overlapping cervical cells is proposed. Our approach is based on linear iterative clustering, thresholding, and support vector machine with eight superpixel-based features to detect the cellular clump regions and the nuclei. Then, a set of procedures (i.e., denoising using antistrophic diffusion filter, histogram equalization, and closing procedure) is utilized to highlight and connect the edges. Finally, overlapping cell segmentation is performed based on edge and region integration using a set of morphological operations.

The proposed technique has been quantitatively evaluated using a dataset of 45 synthetic images with totally 270 cells assembled from real free-lying cervical cells. Our results have proved that the performance of our nuclei detection precedes the performance of the up-to-date techniques. Moreover, our approach has demonstrated a high ability to efficiently segment the cytoplasm of free-lying cells, double overlapping cells, and multiple overlapping cells.

In conclusion, taking into consideration all measures including nuclei and cytoplasm segmentation results and computational time, the proposed technique has proved its practicality and reliability in segmenting complex cervical cells.

Acknowledgment

This work was supported in part by ARC grants.

References

[1] N. Béliz-Osorio, J. Crespo, et al., "Cytology imaging segmentation using the locally constrained watershed transform," in *Mathematical Morphology and Its Applications to Image and Signal Processing*, ed: Springer, 2011, pp. 429-438.

[2] K. Li, Z. Lu, et al., "Cytoplasm and nucleus segmentation in cervical smear images using Radiating GVF Snake," *Patt. Recog.,* vol. 45, pp. 1255-1264, 2012.

[3] M. Hu, X. Ping, et al., "Automated cell nucleus segmentation using improved snake," in *Proc. ICIP 2004*, pp. 2737-2740.

[4] C. Jung and C. Kim, "Segmenting clustered nuclei using H-minima transform-based marker extraction and contour parameterization," *IEEE Trans. Biomed. Eng.,* vol. 57, pp. 2600-2604, 2010.

[5] C. Jung, C. Kim, et al., "Unsupervised segmentation of overlapped nuclei using Bayesian classification," *IEEE Trans. Biomed. Eng.,* vol. 57, pp. 2825-2832, 2010.

[6] M. E. Plissiti and C. Nikou, "Overlapping cell nuclei segmentation using a spatially adaptive active physical model," *IEEE Trans. Img. Proc.,* vol. 21, pp. 4568-4580, 2012.

[7] M. E. Plissiti, C. Nikou, et al., "Automated detection of cell nuclei in pap smear images using morphological reconstruction and clustering," *IEEE Trans. Info. Tech. in Biomed.,* vol. 15, pp. 233-241, 2011.

[8] A. Gençtav, S. Aksoy, et al., "Unsupervised segmentation and classification of cervical cell images," *Patt. Recog.,* vol.45, pp. 4151-68, 2012.

[9] A. Kale and S. Aksoy, "Segmentation of cervical cell images," in *Proc. ICPR 2010*, pp. 2399-2402.

[10] Z. Lu, G. Carneiro, et al., "Automated nucleus and cytoplasm segmentation of overlapping cervical cells," in *Proc. MICCAI 2013*, pp. 452-460.

[11] H.-S. Wu, J. Gil, et al., "Optimal segmentation of cell images," in *IEE Proc.Vis., Img. and Sig. Processing*, 1998, pp. 50-56.

[12] C. H. Lin, Y. K. Chan, et al., "Detection and segmentation of cervical cell cytoplast and nucleus," *Intl. J. Img. Sys. Tech.,* vol.19, pp. 260-270, 2009.

[13] S.-F. Yang-Mao, Y.-K. Chan, et al., "Edge enhancement nucleus and cytoplast contour detector of cervical smear images," *IEEE Trans. Sys., Man, Cyber., Part B: Cybernetics,* vol. 38, pp. 353-366, 2008.

[14] N. A. M. Isa, "Automated edge detection technique for Pap smear images using moving K-means clustering and modified seed based region growing algorithm," *Intl. J. Comp., Internet, Man.,* v.13, pp. 45-59, 2005.

[15] R. Achanta, A. Shaji, et al., "SLIC superpixels," 2010.

[16] Y. Song, W. Cai, et al., "Object localization in medical images based on graphical model with contrast and interest-region terms," in *Proc. CVPR 2012 Workshop on Med. Comp. Vis.*, pp. 1-7.

[17] Y. Song, W. Cai, et al., "Microscopic image segmentation with two-level enhancement of feature discriminability," in *Proc. DICTA 2012*, pp. 1-6.

[18] Y. Song, W. Cai, et al., "Cell nuclei segmentation in fluorescence microscopy images using inter- and intra-region discriminative information," in *Proc. EMBC 2013*, pp. 6087-6090.

[19] Y. Song, W. Cai, et al., "Region-based progressive localization of cell nuclei in microscopic images with data adaptive modeling," *BMC bioinformatics,* vol. 14, p. 173, 2013.

[20] D. Gerónimo, A. López, et al., "Haar wavelets and edge orientation histograms for on–board pedestrian detection," in *Pattern Recognition and Image Analysis*, ed: Springer, 2007, pp. 418-425.

[21] K. Levi and Y. Weiss, "Learning object detection from a small number of examples: the importance of good features," in *Proc. CVPR 2004*, pp. II-53-II-60 Vol. 2.

[22] http://cs.adelaide.edu.au/~carneiro/isbi14_challenge/.